Proton exchange in aqueous urea solutions measured by water-exchange (WEX) NMR spectroscopy and chemical exchange saturation transfer (CEST) imaging in vitro

Julia Stabinska[1], Philipp Neudecker[2, 3], Alexandra Ljimani[1], Hans-Jörg Wittsack[1], Rotem Shlomo Lanzman[1], Anja Müller-Lutz[1]

1 Department of Diagnostic and Interventional Radiology, Medical Faculty, Heinrich Heine University Düsseldorf, Germany

2 Institute of Physical Biology, Heinrich Heine University Düsseldorf, Germany

3 Institute of Complex Systems: Structural Biochemistry (ICS-6), Forschungszentrum Jülich, Germany

***** Corresponding author:

Name	Julia Stabinska
Department	Department of Diagnostic and Interventional Radiology
Institute	Medical Faculty, Heinrich Heine University Düsseldorf
Address	Moorenstr. 5
	40225 Düsseldorf
	Germany
E-mail	Julia.Stabinska@med.uni-duesseldorf.de

Manuscript word count: 4523

Abstract word count: 242

Abstract

Purpose: To characterize the proton exchange in aqueous urea solutions using a modified version of the WEX II filter at high magnetic field, and to assess the feasibility of performing quantitative urea CEST MRI on a 3T clinical MR system.

Methods: In order to study the dependence of the exchange-rate constant k_{sw} of urea as a function of pH and T, the WEX-spectra were acquired at 600 MHz from urea solutions in a pH range from 6.4 to 8.0 and a temperature range from $T = 22°\text{C}$ to $37°\text{C}$. The CEST experiments were performed on a 3T MRI scanner by applying a train of 50 Gaussian-shaped pulses, each 100 ms long with a spacing of 100 ms, for saturation. Exchange rates of urea were calculated using the (extended) AREX metric.

Results: The results showed that proton exchange in aqueous urea solutions is acid- and base catalyzed with the rate constants: $k_a = (9.95 \pm 1.1) \times 10^6$ l/(mol·s) and $k_b = (6.21 \pm 0.21) \times 10^6$ l/(mol·s), respectively. Since the urea protons undergo a slow exchange with water protons, the CEST effect of urea can be observed efficiently at 3T. However, in neutral solutions the exchange rate of urea is minimal and cannot be estimated using the quantitative CEST approach.

Conclusion: By means of the WEX-spectroscopy, the kinetic parameters of the proton exchange in urea solutions have been determined. It was also possible to estimate the exchange rates of urea in a broad range of pH values using the CEST method at a clinical scanner.

Keywords: CEST, urCEST, WEX, urea, proton exchange, exchange rate

Introduction

Urea is the major end-product of protein catabolism and serves an important role in the maintenance of pH homeostasis in mammals (1), (2). It is formed in the liver from ammonia, and later transported in the blood to the kidneys for excretion in the urine (3),(4). Diseases that compromise the function of the kidney are often associated with reduced urea elimination and consequently its increased concentration in blood, as measured by the blood urea nitrogen (BUN) test (5). To assess the structural changes in kidneys, well-established imaging techniques such as ultrasound (US), computed tomography (CT) and magnetic resonance tomography (MRI) are performed. Nevertheless, they usually do not provide adequate functional information (6).

Chemical exchange saturation transfer (CEST) is a novel mechanism of MRI contrast that may overcome this limitation, since it has been shown to be sensitive to the concentrations of the endogenous metabolites and microenviromental properties such as pH and temperature (7), (8), (9), (10). Urea is a potentially attractive CEST agent for in vivo use. Although the normal blood urea level is relatively low (5 – 10 mM), the urea concentration in the urine may be 20 – 100 times higher than in the blood in humans, as reported in (11). Urea is an amide with two $-NH_2$ groups joined by a carbonyl ($C = O$) functional group (12). Already in 1998, Guivel-Sharen et al. identified urea as a major contributor to the kidney/urine chemical exchange at ca. 1 ppm (with water proton frequency defined as 0 ppm) (13). Two years later, Dagher et al. were able to produce a urea distribution map in vivo at 1.5 T using CEST MRI (14). Apart from an ISMRM abstract in 2015 (15), no further studies on urea-weighted CEST (urCEST) at a clinical MRI system have been published.

Knowledge about the chemical shift, exchange rate and relaxation properties of urea leads to better understanding of the saturation transfer effects in the human kidney in vivo. Because many kidney diseases alter pH and urea gradients in kidney, an implementation of pH-sensitive CEST imaging might be of great interest particularly in the clinical context (7), (16). In this study, we characterize the proton exchange properties of urea with water using water exchange spectroscopy (WEX II) (17) at ultra-high magnetic field, and evaluate the feasibility of performing quantitative urea CEST analysis at 3T. In particular, we determine the chemical exchange rates k_{sw} between urea amide protons s and water w as a function of pH, concentration and temperature by means of WEX spectroscopy and CEST experiments.

Moreover, in order to examine the specificity of the urea-weighted CEST imaging in kidney, we

study the CEST effect of other important kidney metabolites, e.g creatinine, ammonia, hippuric acid and citric acid at different pH values (18), (19). Eventually, we investigate the contribution of the urCEST to the total CEST effect in urine.

Methods

Preparation of the aqueous urea solutions

For WEX experiments, six aqueous model solutions containing 250 mM urea ($\geq$ 99.5% cryst. urea, Carl Roth, Karlsruhe, Germany), 50 mM sodium/potassium phosphate buffer ($\geq$ 99% disodium hydrogen phosphate and $\geq$ 99.5% potassium dihydrogen phosphate, Carl Roth, Karlsruhe, Germany) and 5% (v/v) deuterium oxide (D_2O, 99.8 atom % D, Carl Roth, Karlsruhe, Germany) for the field-frequency lock were prepared at different pH = (6.39, 6.56, 6.96, 7.38, 7.72, 7.97) and measured at temperature T = 37.0°C. The samples with pH = 6.56 and pH = 7.97 were additionally measured at varied temperatures T = (22.0°C, 27.0°C, 32.0°C, 37.0°C).

For CEST studies, sixteen 50 ml aqueous solutions with 250 mM urea concentration were mixed with 50 mM Na/K phosphate buffer at pH = (5.66, 5.72, 5.93, 6.12, 6.20, 6.37, 6.54, 6.86, 7.00, 7.20, 7.37, 7.65, 7.80, 8.02, 8.20, 8.41). In addition, four samples containing different urea concentration c_s = (10 mM, 25 mM, 50 mM, 100 mM) at pH 7.60 were prepared.

The other studied metabolites were: creatinine, ammonia, hippuric acid, citric acid, taurine, creatine, histidine, glucose, glutamine, myo-inositol, alanine, lysine, allantoin, threonine, lactate, sorbitol, glutamic acid, choline and glycogen. The concentration of most compounds was 100 mM, and the remainder determined by their solubility in the sample buffer. Each phantom consisted of four tubes containing model solution dissolved in 50 mM Na/K phosphate buffer at pH = (6.2, 6.6, 7.0, 7.4). Additionally, individual and mixed aqueous solutions of 180 mM urea, 15 mM creatinine and 1 mM creatine, corresponding to the normal concentrations of these metabolites in urine, were prepared. In addition, an urine sample was collected from a healthy volunteer.The pH value of the model mixture and the urine sample were: 5.97 and 5.90 at T = 37°C, respectively.

The temperature of the model solutions during the measurements was kept constant $T = (37 \pm 1)$°C by using an MR-compatible cooling box.

WEX experiments

The WEX spectra were acquired on a Bruker Avance III HD 600 MHz NMR spectrometer (Bruker, Ettlingen, Germany) equipped with a cryogenically cooled quadruple resonance probe with z-axis pulsed field gradient capabilities. The sample temperature was calibrated using methanol-d_4 (20). The exchange of water protons with urea was monitored with the pulse sequence shown in Figure 1 using 33 different mixing times (T_m) ranging from 20 ms to 2000 ms. For each mixing time, 32 transients were recorded with a recycle delay of 4.7 s. The resulting spectra were processed using NMRPipe and NMRDraw (21) and the ^{1}H resonance of urea was integrated.

CEST experiments

All CEST experiments were performed on the 3T whole body MR clinical scanners (Magnetom Trio and Magnetom Prisma, Siemens Healthineers, Erlangen, Germany). Z-spectra were obtained using presaturated gradient-echo imaging with the following parameters: FOV = 130 x 130 mm^2, matrix size: 128 x 128, slice thickness = 5.0 mm, repetition time T_R = 7.7 ms and echo time T_E = 3.61 ms. In the urCEST experiments, presaturation was achieved using 50 Gaussian-shaped pulses with low RF saturation power of B_1 = 1.0 μ T, pulse duration t_{pd} = 100 ms and inter-pulse delay t_{ipd} = 100 ms (duty cycle DC = 50%, total saturation time T_{sat} = 9.9 s). Forty-three saturated images at evenly distributed frequency offsets between ± 4 ppm and an unsaturated image at 300 ppm were acquired. To determine B_0 maps using the water saturation shift referencing method (WASSR) (22), a single Gaussian-shaped pulse with RF saturation power of B_1 = 0.1 μT and pulse duration t_{pd} = 56 ms was applied. The WASSR z-spectra were obtained at 42 offsets between -1 ppm and 1 ppm. Additionally, T1-weighted images were measured by a turbo-inversion-recovery sequence. Altogether, twelve contrasts at different inversion delays (TI) ranging from 25 ms to 5 s were fitted to calculate T_1 maps. The same measurement protocol was applied to acquire the CEST signals in the phantom including mixed solution of urea, creatinine and creatine as well as in the urine sample.

Further phantom experiments were performed using 20 Gaussian-shaped pulses with three different RF amplitudes, $B1 = (0.8, 1.2, 1.6)\mu$T and pulse duration $t_{pd} = t_{ipd}$ = 100 ms. Z-spectra were acquired at 45 frequency offsets between -6 and 6 ppm.

Data analysis

Post-processing was performed using in house written programs in MATLAB (Mathworks, Natick, Massachusetts, USA). The T_1 maps were obtained by pixel-by-pixel least-squares fitting of the signal equation $I = I_0 \cdot [1 - 2 \cdot exp(-TI/T_1)]$, where I is the signal intensity and TI is the inversion time. The exchange rates of urea were calculated as described in the following sections.

Determination of k_a and k_b for urea by WEX

As in standard amides, proton exchange in urea solutions is acid- and base-catalyzed and therefore strongly pH dependent (23) (24):

$$\mathrm{k_{sw}} = \mathrm{k_b} \cdot 10^{\mathrm{pH-pK_w}} + \mathrm{k_a} \cdot 10^{-\mathrm{pH}} + \mathrm{k_0} \qquad [1]$$

where k_b, k_a and k_0 (in l/(mol·s)) are rate constants for the base-, acid- and water-catalyzed protolysis, respectively. The rate of the spontaneous reaction (k_0) is very slow compared to acid and based catalysis, and thus assumed to be negligible (24). The pK_w refers to the negative decadic logarithm of the ionization constant, which is temperature dependent according to the solution of the van't Hoff equation (25) (26):

$$\mathrm{pK_w(T)} = \mathrm{pK_w(T_0)} - (\frac{\mathrm{\Delta H^0_R}}{\mathrm{R} \cdot \ln(10)})(\frac{1}{\mathrm{T_0}} - \frac{1}{\mathrm{T}}) \qquad [2]$$

$pK_w(T_0)$ here refers to the logarithm of the water-ion product at temperature T_0 = 25°C, ΔH^0_R = 55.84 kJ/mol is the standard reaction enthalpy for the self-dissociation of water and R = 8.314 J/(mol K) is the gas constant (25), (26). Thus, we assumed pK_w = 13.617 at T = 37°C. The urea signal intensity $S_s(T_m)$ as a function of the mixing time T_m is given by (26):

$$\mathrm{S_s(T_m)} = \underbrace{\frac{k_{ws} M_{zw}(0)}{k_{sw} + R_{1s} - R1w}}_{\mathrm{C}} [\mathrm{e}^{-\mathrm{R_{1w}} \cdot (\mathrm{T_m} - \mathrm{T_{WFB}})} - \mathrm{e}^{-(\mathrm{k_{sw}} + \mathrm{R1s}) \cdot (\mathrm{T_m} - \mathrm{T_{WFB}})}] \qquad [3]$$

where R_{1w}, R_{1s} are the longitudinal relaxation rates of the water and solute pool, respectively; k_{sw} is the chemical exchange rate between solute s and water pool w and k_{ws} is the back-exchange rate; $M_{zw}(0)$ is the z magnetization of the water protons at the beginning of the mixing period. The $k_{sw} + R_{1s}$ values were obtained from a fit of Equation 4 to the measured urea signal integrals $Ss(T_m - T_{WFB})$ at any given pH and temperature in MATLAB, where TWFB is a variable fitting parameter introduced to account for the effects of the water flip-back pulse at the end of the mixing

period (see below). Eventually, the k_b and k_a rates at given temperature were estimated by bi-exponential fit of the measured $k_{sw} + R_{1s}$ values with the following equation:

$$\mathrm{k_{sw} + R_{1s} = k_b \cdot 10^{pH-pK_w} + 10^{-pH} + R_{1s}} \quad [4]$$

Furthermore, the activation energies $E_{A,b}$ and $E_{A,a}$ of, respectively, base- and acid-catalyzed reactions were calculated by fitting the measured $k_{sw} + R_{1s}$ values at pH 7.97 and pH 6.56 as a function of temperature. It was assumed that at pH 7.97, the proton exchange with water is dominantly base-catalyzed, hence (27):

$$\mathrm{k_{sw} + R_{1s} = k_b(310.15K) \cdot [\frac{mol}{l}] \cdot 10^{pH-14+\frac{\Delta H^0_R}{R\cdot ln(10)}(\frac{1}{298.15K}-\frac{1}{T})+\frac{E_{A,b}}{R\cdot ln(10)}(\frac{1}{310.15}-\frac{1}{T})} + R_{1s}} \quad [5]$$

Similarly, at pH 6.56, the exchange process between water and amide protons of urea is mainly acid-catalyzed, and thus (27):

$$\mathrm{k_{sw} + R_{1s} = k_a(310.15K) \cdot [\frac{mol}{l}] \cdot 10^{-pH+\frac{E_{A,a}}{R\cdot ln(10)}(\frac{1}{310.15}-\frac{1}{T})} + R_{1s}} \quad [6]$$

where $k_b(310.15K)$ and $k_a(310.15K)$ are the obtained rate constants at $T = 310.15$ K. The R_{1s} was assumed to be independent of temperature (27).

Determination of k_{sw} for urea by CEST

Recently, several theoretical approaches of quantifying proton exchange rates from data obtained in CEST experiments were proposed (28) (29) (30) (31) (32) (33). Especially, a novel magnetization transfer (MT) ratio called MTR_{Rex}, which eliminates spillover effect and semi-solid macromolecular magnetization transfer, was introduced by Zaiss et al. (34):

$$\mathrm{MTR_{Rex} = \frac{1}{Z_{lab}} - \frac{1}{Z_{ref}} = \frac{R_{ex} \cdot DC}{R_{1w}}} \quad [7]$$

where $Z_{lab} = Z(+\Delta\omega)$ is the label scan around the resonance of the CEST pool s, $Z_{ref} = Z(-\Delta\omega)$, the reference scan at the opposite frequency with respect to water, R_{ex} refers to the exchange-dependent relaxation in the rotating frame and R_{1w}, is the relaxation rate of the water pool w. Duty cycle, $DC = t_{pd}/(t_{ipd} + t_{pd})$, is determined by the pulse duration t_{pd} and the inter-pulse delay t_{ipd}. The MTR_{Rex} metric can be extended to an apparent exchange-dependent relaxation metric, –$AREX$:

$$AREX = MTR_{Rex} \cdot R_{1w} \quad [8]$$

More recently Roeloffs et al. demonstrated that in the case of exchange rates that are small with respect to the inter-pulse delay, modeling magnetization transfer during the pauses between the RF pulses might be crucial (35). In their theoretical model, they assume bi-exponential dynamics of the magnetization in the water pool during the inter-pulse delay (ISAR2), instead of a mono-exponential recovery with rate R_{1w} (ISAR1), as had been previously presumed (36). As a result, the MTR_{rex} metric has to be extended by an additional term (35):

$$\mathrm{MTR_{Rex}} = \frac{1}{\mathrm{Z_{lab}}} - \frac{1}{\mathrm{Z_{ref}}} = \frac{\mathrm{R_{ex}} \cdot \mathrm{DC}}{\mathrm{R_{1w}}} \cdot (1 + \frac{1 - \mathrm{R_{1w}} \mathrm{t_{ipd}}}{\mathrm{t_{pd}} \mathrm{k_{sw}}}) \quad [9]$$

In the large shift limit (LS) (i) $\delta\omega_s \to \infty$ and in the full saturation limit (FS) (ii) $\omega_1 \gg R_{2s} + k_{sw}$, when applying RF pulse at the CEST pool s resonance, $R_{ex} = f_s \cdot k_{sw}$ and hence (34):

$$\mathrm{k_{sw}} = \frac{\mathrm{MTR_{Rex}} \cdot \mathrm{R_{1w}}}{\mathrm{DC} \cdot \mathrm{f_s}} \quad [10]$$

where k_{sw} describes the exchange rate of urea, f_s the proton fraction (see below), R_{2s} the transverse relaxation rate of the CEST pool s, ω_1 the RF irradiation amplitude and $\delta\omega_s$ corresponds to the frequency offset of pool s. The proton fraction is given by (34):

$$\mathrm{f_s} = \frac{\mathrm{n_s}}{\mathrm{n_w}} \cdot \frac{\mathrm{c_s}}{\mathrm{c_w}} \quad [11]$$

c_i and n_i are the concentration and number of exchangeable protons per molecule of pool i ($i = s$ or w). It is assumed that $c_w = 55$ M and $n_w = 2$.

Results

Implementation of the WEX II pulse sequence

For the measurement of water exchange rates we used a phase-cycled difference experiment based on water-selective inversion using the WEX II filter sequence with a 1D ^{1}H read-out as described by Mori et al. (17). Because the broad ^{1}H resonance of urea (5.45 $\cdots$ 6.05 ppm) is separated from the ^1H_2O resonance (between 4.66 ppm and 4.80 ppm in the temperature range studied here) by only 0.65 ppm (390 Hz at 600 MHz) (Figure 2), such an experiment requires not only highly frequency-selective water inversion but also a 1D ^{1}H read-out with excellent water suppression with water flip-back, a uniform excitation profile with an extremely narrow transition region near the ^1H_2O resonance, and an exceptionally flat baseline. To this end, the 3-9-19-WATERGATE water suppression scheme used in the original WEX II sequence (17) was replaced by an excitation

sculpting (37) read-out with water flip-back (38) (Figure 1). Water-selective excitation and water flip-back was achieved by 12.0 ms self-refocusing E-BURP-1 (39) 90° pulses, water-selective refocusing by 4.0 ms 180° pulses with a shape corresponding to the central lobe of a sinc(x) = sin(x)/x function. Simulations based on the Bloch equations and control experiments were used to establish that these pulses are sufficiently frequency-selective that their effect on the ^{1}H resonance of urea is negligible. In brief, the initial combination of water-selective and hard 90° pulses in Figure 1 selectively aligns the water magnetization along either the negative (-z) or the positive (+z) longitudinal axis in successive transients. Solute magnetization is rotated into the transverse plane and dephased by the crushing gradient G_1. The differential transfer of the (negative or positive) longitudinal magnetization of water protons to other metabolites during the mixing time, T_m, in successive scans is obtained by phase cycling the pulses of the WEX II filter together with the receiver (17). A weak gradient (G_2) is applied during the mixing time to prevent radiation damping (17). Any longitudinal magnetization transferred to the solute is then detected with a 1D ^{1}H pulse sequence with excitation sculpting (37) preceded by a water flip-back pulse (38) to achieve excellent water suppression and a very flat spectral baseline (Figure 2). While this sequence preserves most of the salient features of the original WEX II sequence (17), we prefer to apply the long (12.0 ms) water flip-back pulse at the end of T_m before the hard 90° read-out pulse in order to keep the excitation sculpting gradient double echo short enough to limit transverse relaxation and any homonuclear scalar coupling evolution. As a result of the complex trajectory of the water magnetization during this water flip-back pulse, the effective mixing time is somewhat shorter than T_m and no longer known a priori, but has to be corrected a posteriori by a variable parameter during data analysis. An important technical consideration – especially on modern high-field instruments with highly sensitive cryoprobes – is the effect of radiation damping, which opposes water-selective pulses that rotate the magnetization away from the positive longitudinal axis ("flip-down") but reinforces water-selective pulses that rotate the magnetization towards the positive longitudinal axis ("flip-up"). As a result, flip-down and flip-up water-selective pulses are significantly different and have to be calibrated independently (40). The water-selective WEX II excitation pulse in Figure 1 has to be calibrated as a flip-down pulse because it rotates the magnetization from the positive (+z) longitudinal axis into the transverse plane. By contrast, the water flip-back pulse at the end of T_m (hatched in Figure 1) rotates the magnetization from either –z or +z into the transverse plane and therefore alternates between a flip-up and flip-down pulse, respectively, in successive transients. If only flip-down pulses are used for the sake of convenience, water flip-back will be incomplete and

it is important to choose a recycle delay long enough for longitudinal relaxation of ^1H_2O between successive transients. As an alternative to the 1D ^{1}H read-out presented in Figure 1, it is also straightforward to take advantage of the much sharper linewidth of the $^{15}NH_2$ groups of urea at natural abundance by combining the WEX II filter with a [^{1}H,^{15}N] HSQC read-out sequence with gradient coherence selection and water flip-back (41) if the signal to noise ratio is not limiting.

Determination of the exchange rate constants k_a and k_b and the activation energies $E_{A,a}$ and $E_{A,b}$ of urea by WEX

The chemical shift of the urea amide protons in the WEX spectra is $\delta = 5.73$ ppm at pH 6.96 and $T = 37.0$°C. The experimentally determined signal intensities of urea are in an excellent agreement with the fitted function $S_s(T_m)$(Equation 3) (Figure 3) proven by mean fit quality of $R^2 = 1.0$ (42). Similarly, the $k_{sw} + R_{1s}$ values obtained from six measured samples at different pH match well the fitted function $k_{sw}(pH) + R_{1s}$ (Equation 4) (Table 1, Figure 4). With a fit quality of $R^2 = 0.996$, the estimated acid- and base- catalyzed exchange rate constants of urea at 37.0°C (310.15 K) are $k_a = (9.95 \pm 1.11) \times 10^6$ l/(mol·s) and $k_b = (6.21 \pm 0.21) \times 10^6$ l/(mol·s), respectively. The assumption of bi-exponential dependence of the urea exchange rate on pH is thus clearly verified. It is worth noting that the acid-catalyzed rate constant is much faster than the base-catalyzed rate constant. Using the calculated k_a and k_b values, it is possible to extrapolate the k_{sw} for any pH value (Table 2).

The activation energies for base- and acid-catalyzed proton exchange in urea solution are $E_{A,b} = 43.52 \pm 9.56$ kJ/mol (quality of the fit: R^2 =0.995) and $E_{A,a} = 79.13 \pm 15.87$ kJ/mol (quality of the fit: $R^2 = 0.975$). The Arrhenius plot ($ln(k_{sw})$ against $1/T$) gives, as expected, a straight line (Figure 4).

Determination of the exchange rates k_{sw} of urea by CEST

The CEST peak from urea is located at ca. 1 ppm with respect to the water resonance, which is arbitrarily set at 0 ppm. After correction of the MTR_{Rex} data for effects of T_1 relaxation (by multiplying with the R_{1w} maps), we obtained the apparent exchange-related relaxation metric (AREX) (Equation 8). The bi-exponential dependence of the AREX values on pH confirms that the proton exchange in aqueous urea solutions is acid- and base- catalyzed (Figure 5). By varying the urea concentration c_s at fixed pH = 8.04 and $T = (37 \pm 1)$°C, we could also demonstrate that the (corrected) AREX is linearly proportional to the urea concentration ($R^2 = 0.991$) (Figure 5).

Using Equation 11 and the $k_{sw,ref}$ values determined by extrapolation of Equation 4 with the rate constants k_a and k_b measured by means of WEX spectroscopy, we were able to calculate the proton fraction f_s and thus the number of labile protons in urea n_s (Equation 11). Using the AREX maps of eight model solutions at pH = (5.66, 5.72, 5.92, 6.12, 7.8, 8.02, 8.20, 8.41), we obtained n_s = 4.10 ± 0.21. This result suggests that urea possesses four labile protons. Finally, employing the Equation 10 with $f_s = 4$, the exchange rate k_{sw} maps of urea can be calculated (Figure 5). The k_{sw} derived experimentally from CEST data agree well with the reference values $k_{sw,ref}$, at pH values below 6.2 and above 7.4 at 37°C (Figure 5, Table 2). In the neutral solutions the exchange rate of urea is minimal and could not be accurately estimated from the CEST data. In general, it is possible to determine the pH maps by solving the Equation 1 with the k_{sw} values calculated from the CEST data. However, in the case of bi-exponential function we obtain two real solutions and without additional information, we cannot univocally decide which of the two possible pH values is "correct".

Assessment of pH-dependence of the CEST effect of other kidney metabolites

In order to identify major kidney metabolites, which possess exchangeable protons and may generate an experimentally measurable CEST effect under physiological condition, results from animal (18) and human studies (43) on kidney tissues as well as the Urine Metabolome Database (19) were analyzed. Only molecules found in relatively high abundance in kidney tissue and urine were investigated. Finally, a comprehensive list of the potential CEST-active metabolites was created (Table 3). The z-spectra and magnetization transfer ratio asymmetry (MTR_{asym}) curves were measured at various pH values. While all of the systematically tested metabolites possess exchangeable protons, not all of them generate large CEST contrast at 3T in the measured pH range of 6.2-7.4 and temperature T = 37°C (z-spectra and MTR_{asym} curves not shown). Creatinine, creatine, glutamine, alanine, allantoin and glutamate showed the highest CEST effect under physiological conditions (Figure 6).

Investigation of the specificity of urea-weighted CEST imaging

To examine the specificity of urCEST, aqueous solutions containing three most abundant urine metabolites that show measurable CEST effect, namely urea, creatinine and creatine, were prepared at pH 5.97 and measured at T = 37°C (Figure 7). The concentrations of the individual compounds were: 180 mM, 15 mM and 1 mM for urea, creatinine and creatine, respectively, corresponding to

the normal concentrations of these metabolites in urine (Table 3). The determined exchange rate of urea was: $k_{sw} = 9.25 \pm 1.79$, indicating good agreement with the reference k_{sw} value ($k_{sw} = 10.80 \pm 1.13$). Moreover, the calculated z-spectrum and the MTR_{asym} curve of the mixed phantom were similar to those obtained in the urine sample at pH 5.90. Both CEST spectra reveal a dominant peak at ca. 1 ppm, which can be assigned to the exchanging amide protons of urea.

Discussion

Proton exchange in aqueous urea solutions

In our study we were able to determine experimentally the urea exchange rate constants with high accuracy. The previously reported rate constants of urea are: $k_a = (7.0 \pm 2.0) \times 10^6$ l/(mol·s), $k_b = (4.8 \pm 1.6) \times 10^6$ l/(mol·s) at T = 22°C (29), and $k_a = (9.0 \pm 1.0) \times 10^6$ l/(mol·s), $k_b = (2.4 \pm 1.0) \times 10^6$ l/(mol·s) at $T = 35$°C (24) (44) and have been measured by use of line shapes of urea and water in ^{1}H NMR. For amides, this method is not exact because of line broadening associated with ^{14}N quadrupole relaxation of the amide nitrogen (45). As an alternative, line shapes for the proton-coupled ^{15}N NMR spectra were calculated for investigating the NH-exchange rates of urea, yielding the following results: $k_a = (18.0 \pm 12.0) \times 10^6$ l/(mol·s), $k_b = (4.4 \pm 1.0) \times 10^6$ l/(mol·s) at $T = 32$°C (45). It seems that the WEX II method provides smaller standard errors than the linewidth-based methods and thus improves the accuracy and precision of predictions. Although all previous estimated k_a and k_b values are in good agreement, direct comparison of the results is difficult due to differences in the experimental conditions, such as the buffer concentration and temperature. Since the pH in urea solutions tends to drift slowly because of CO_2 absorption and decomposition of urea into ammonium and cyanate ions (24) (46), we dissolved urea in 50 mM Na/K-phosphate buffer. The pH value did not change over a period of several hours.

The acid-catalyzed rate constant of urea is large compared to rate constants for acid-catalyzed protolysis of most amides (23) (44). High k_a rate constant suggests higher probability of H_3O^+ with nitrogen than with oxygen, resulting in observable proton transfer(44). Thus, the large value of k_a for urea solution implies protonation on urea nitrogen rather than oxygen (44).

The comparison of the estimated activation energies $E_{A,a} \approx (19 \pm 4)$ kcal/mol and $E_{A,b} \approx (10 \pm 2)$ kcal/mol with the apparent heat of activation for amide hydrogen exchange of about 17 kcal/mol, reported by Englander et al., shows good agreement (47). Recently, Bodet et al. estimated the effective activation energy of amide proton exchange $E_{b,eff} = (54.12 \pm 9.15)$ kJ/mol $\approx (13 \pm 2)$

kcal/mol in carnosine solutions buffered with (1/15) M PBS buffer (27). The same study also showed that the buffer has a strong influence on the amide hydrogen exchange rate and its dependence on pH and temperature. This finding should be taken into consideration when analysing our results.

WEX and CEST methods

Several methods have been proposed for estimation exchange rates, which is possible due to their dependence on the saturation power and time (29) (31) (48) (49) (32) (33) (50). The water exchange (WEX) filter sequence has already been used for measuring exchange rates of slowly exchanging species (17) (27) (37). Therefore, we decided to apply this method to amide exchange in aqueous urea solutions. In contrast to the original WEX II sequence, we use excitation sculpting instead of WATERGATE technique for water suppression. Because of the large width of the urea peak and its nearness to the water resonant frequency, we expect that the WATERGATE water suppression may negatively impact the urea signal due to lack of sufficient selectivity (51). One of the challenges with the spectroscopy (MRS) based methods, such as the WEX approach, is the low sensitivity, which makes it difficult to detect low abundance metabolites in vivo. Furthermore, the WEX experiments are not suitable for measuring faster rates since the signal of the exchangeable peak is reduced owing to exchange with suppressed water protons (28) (52). The WEX spectroscopy has been already used to measure exchange rates of creatine guanidinium protons and amide protons of carnosine on a 3T clinical MRI system (26) (27). However, this method is not applicable to urea samples at low magnetic field.

The exchange rates of urea derived from CEST experiments are in good agreement with those obtained by WEX experiments. However, it was not possible to determine the k_{sw} values of urea in the physiologically relevant pH range. Derivation of the exchange-dependent relaxation rate R_{ex} used here is based on the assumption that the influence of the R_{1s} is negligible against k_{sw} for exchanging system (53) (54). This requirement is not fulfilled for exchange rates that are in the order of the longitudinal relaxation rate R_{1s}. Moreover, in the neutral solutions the CEST effect was minimal and thus the signal to noise ratio was insufficient for a proper quantification.

In order to determine the quantitative CEST parameters of urea we have applied the extended steady-state method AREX, introduced by Roelloffs et al. (34) (35). For extremely slow exchange rates of urea, modelling of bi-exponential decay during the break was important. The exchange rates obtained using the "standard" AREX approach, were significantly overestimated (approximately 40%). Since the CEST contrast depends on both concentration and k_sw, it is necessary to employ

quantitative methods that allow separating these parameters. Previous study have shown that the CEST effect can be represented as a linear function of $1/B_1^2$ and that the exchange rate and proton fraction can be determined independently by linear regression (the so-called Ω-plot) (31) (48) (49) (32) (33). However, this method seems to be not applicable at low exchange rates due to a high noise level and small B_1 dispersion (26) (55).

In our study, we have investigated a number of important kidney/urine metabolites with exchangeable protons that may produce a CEST effect in vivo. However, for most of them no CEST contrast in the examined pH range and at a buffer concentration of 50 mM was observed at 37°C. This is consistent with the fast exchange. Moreover, in the case of hydroxyl groups of e.g. myo-inositol, glucose, and glycogen the resonance peaks were possibly within the linewidth of the water resonance.Therefore, it is unlikely that any of these metabolites contribute to the total CEST effect at ca. 1 ppm in kidney at clinical field. Besides urea, several other compounds show a measurable CEST effect under physiological conditions at 3T. These might potentially overlap with the urea CEST signal in the urine/kidney in vivo. The absolute urea quantification might be, therefore, considerably hampered. In our study, we were able to estimate the k_{sw} of urea from CEST experiments performed on a mixture model solution of urea, creatinine and creatine. However, we have assumed that the urea concentration is much higher than the creatinine concentration (12:1), as had been previously measured in urine (Table 3) (19). The difference in MTR_{asym} between the urine and mixture peaks results most likely from slightly different pH values as well as different concentrations of individual metabolites in urine compared with the mixed solution. To the best of our knowledge, no study determined absolute concentrations of metabolites in human kidney in vivo. Further extensive research is necessary in order to assess the contribution of other kidney metabolites superimposed on the urCEST effect at different pH.

pH-sensitive chemical exchange saturation transfer (CEST) MRI is a promising new method for in vivo applications (56) (57) (58) (59) (60). Exogenous CEST agent pH mapping have already been applied for kidney imaging. The measured pH in kidneys was shown to vary between 5.4 and 7.4 for healthy mice (58). Since the exchange rate of urea is minimal at this pH range, it might be challenging to obtain the pH maps of kidneys using only the quantitative urea-weighted CEST method. On the other hand, pH could be measured independently using paraCEST (e.g. Lanthanide-DOTA-tetraamide complexes (56), Eu3+ based agents (56) (57)) or diaCEST agents (e.g. Iopamidol (58), (59)) in order to derive urea concentration by combining Equation [1] and equation [10] (60).

Conclusions

In our study, we present a successful application of the WEX spectroscopy for determining exchange rate constants of urea and evaluate the feasibility of the quantitative urea-weighted CEST imaging at a clinical MRI system. We show that similar to simple amides, proton exchange in aqueous urea solutions is acid- and base-catalyzed with the rate constants: $k_a = (9.95 \pm 1.1) \times 10^6$ l/(mol·s) and $k_b = (6.21 \pm 0.21) \times 10^6$ l/(mol·s), and activation energies: $E_{A,a} = 79.13 \pm 15.87$ kJ/mol and $E_{A,b} = 43.52 \pm 9.56$ kJ/mol, respectively. Although urea protons undergo a slow exchange with water protons, it was possible to estimate its exchange rate at pH values below 6.2 and above 7.4 at $T = (37 \pm 1)$°C using the quantitative CEST analysis. Moreover, several other kidney metabolites, which are expected to partially conceal the CEST effect of urea in vivo, were examined. Further investigations are needed to characterize the explicit dependence of the exchange rate constant of urea amide protons on different pH buffer systems.

Acknowledgments

This study was supported by a Grant from the Forschungskommission of the Faculty of Medicine, Heinrich-Heine-University, Düsseldorf (Grant No: 13/2015). The authors acknowledge access to the Jülich-Düsseldorf Biomolecular NMR Center.

References

1 Bennion Brian J, Daggett Valerie. The molecular basis for the chemical denaturation of proteins by urea. *Proceedings of the National Academy of Sciences of the United States of America.* 2003;100:5142–7.

2 Atkinson Daniel E., Bourke Edmund. The role of ureagenesis in pH homeostasis *Trends in Biochemical Sciences.* 1984;9:297–300.

3 Weiner I David, Mitch William E, Sands Jeff M. Urea and Ammonia Metabolism and the Control of Renal Nitrogen Excretion *Clinical Journal of the American Society of Nephrology : CJASN.* 2015;10:1444–1458.

4 Champe Pamela C., Harvey Richard A., Ferrier Denise R.. *Lippincott's Illustrated Reviews: Biochemistry.* . Philadelphia: Lippincott Williams & Wilkins5th ed. 2004.

5 Baum Neil, Dichoso Carmelo C., Carlton C.Eugene. Blood urea nitrogen and serum creatinine: Physiology and interpretations *Urology.* 1975;5:583–588.

6 Herget-Rosenthal Stefan. Imaging Techniques in the Management of Chronic Kidney Disease: Current Developments and Future Perspectives *Seminars in Nephrology.* 2011;31:283–290.

7 Ward K.M, Aletras A.H, Balaban R.S. A New Class of Contrast Agents for MRI Based on Proton Chemical Exchange Dependent Saturation Transfer (CEST) *Journal of Magnetic Resonance.* 2000;143:79–87.

8 Zijl Peter C M, Yadav Nirbhay N. Chemical exchange saturation transfer (CEST): What is in a name and what isn't? *Magnetic Resonance in Medicine.* 2011;65:927–948.

9 Heo Hye-Young, Zhang Yi, Burton Tina M, et al. Improving the detection sensitivity of pH-weighted amide proton transfer MRI in acute stroke patients using extrapolated semisolid magnetization transfer reference signals *Magnetic Resonance in Medicine.* 2017;78:871–880.

10 Zhang Shanrong, Malloy Craig R, Sherry A Dean. MRI Thermometry Based on PARACEST Agents *Journal of the American Chemical Society.* 2005;127:17572–17573.

11 Yang Baoxue, Bankir Lise. Urea and urine concentrating ability: new insights from studies in mice *American Journal of Physiology-Renal Physiology.* 2005;288:F881-F896.

12 Hastings Janna, Matos Paula, Dekker Adriano, et al. The ChEBI reference database and ontology for biologically relevant chemistry: enhancements for 2013 *Nucleic Acids Research.* 2013;41:D456-D463.

13 Guivel-Scharen V., Sinnwell T., Wolff S.D., Balaban R.S.. Detection of Proton Chemical Exchange between Metabolites and Water in Biological Tissues *Journal of Magnetic Resonance.* 1998;133:36–45.

14 Dagher Azar P, Aletras Anthony, Choyke Peter, Balaban Robert S. Imaging of urea using chemical exchange-dependent saturation transfer at 1.5T *Journal of Magnetic Resonance Imaging.* 2000;12:745–748.

15 Vinogradov Elena, Liu Zheng, Madhuranthakarn Ananth, et al. Endogenous urea CEST (urCEST) for MRI monitoring of kidney function in *Proceedings of the International Society for Magnetic Resonance in Medicine* 2015.

16 Kim Jinsuh, Wu Yin, Guo Yingkun, Zheng Hairong, Sun Phillip Zhe. A review of optimization and quantification techniques for chemical exchange saturation transfer MRI toward sensitive in vivo imaging *Contrast Media & Molecular Imaging.* 2015;10:163–178.

17 Mori Susumu, Abeygunawardana Chitrananda, Zijl Peter C.M., Berg Jeremy M.. Water Exchange Filter with Improved Sensitivity (WEX II) to Study Solvent-Exchangeable Protons. Application to the Consensus Zinc Finger Peptide CP-1 *Journal of Magnetic Resonance, Series B.* 1996;110:96–101.

18 Serkova Natalie, Florian Fuller T., Klawitter Jost, Freise Chris E., Niemann Claus U.. 1H-NMR–based metabolic signatures of mild and severe ischemia/reperfusion injury in rat kidney transplants *Kidney International.* 2005;67:1142–1151.

19 Bouatra Souhaila, Aziat Farid, Mandal Rupasri, et al. The Human Urine Metabolome *PLoS ONE.* 2013;8:e73076.

20 Findeisen M, Brand T, Berger S. A 1H-NMR thermometer suitable for cryoprobes *Magnetic Resonance in Chemistry.* 2006;45:175–178.

21 Delaglio Frank, Grzesiek Stephan, Vuister Geerten, Zhu Guang, Pfeifer John, Bax Ad. NMRPipe: A multidimensional spectral processing system based on UNIX pipes *Journal of Biomolecular NMR.* 1995;6:277–293.

22 Kim Mina, Gillen Joseph, Landman Bennett A, Zhou Jinyuan, Zijl Peter C M. Water saturation shift referencing (WASSR) for chemical exchange saturation transfer (CEST) experiments *Magnetic Resonance in Medicine.* 2009;61:1441–1450.

23 Berger A, Loewenstein A, Meiboom S. Nuclear Magnetic Resonance Study of the Protolysis and Ionization of N-Methylacetamide1 *Journal of the American Chemical Society.* 1959;81:62–67.

24 Klotz Irving M, Hunston Donald L. Proton exchange in aqueous urea solutions *The Journal of Physical Chemistry.* 1971;75:2123–2127.

25 Foote H. W.. Elements of Physical Chemistry *Science.* 1907;26:588–588.

26 Goerke Steffen, Zaiss Moritz, Bachert Peter. Characterization of creatine guanidinium proton exchange by water-exchange (WEX) spectroscopy for absolute-pH CEST imaging in vitro *NMR in Biomedicine.* 2014;27:507–518.

27 Bodet Olga, Goerke Steffen, Behl Nicolas G R, Roeloffs Volkert, Zaiss Moritz, Bachert Peter. Amide proton transfer of carnosine in aqueous solution studied in vitro by WEX and CEST experiments *NMR in Biomedicine.* 2015;28:1097–1103.

28 McMahon Michael T, Gilad Assaf A, Zhou Jinyuan, Sun Phillip Z, Bulte Jeff W M, Zijl Peter C M. Quantifying exchange rates in chemical exchange saturation transfer agents using the saturation time and saturation power dependencies of the magnetization transfer effect on the magnetic resonance imaging signal (QUEST and QUESP): Ph calibration for poly-L-lysine and a starburst dendrimer *Magnetic Resonance in Medicine.* 2006;55:836–847.

29 Dixon W Thomas, Ren Jimin, Lubag Angelo J M, et al. A concentration-independent method to measure exchange rates in PARACEST agents *Magnetic Resonance in Medicine.* 2010;63:625–632.

30 Sun Phillip Zhe. Simplified quantification of labile proton concentration-weighted chemical exchange rate (kws) with RF saturation time dependent ratiometric analysis (QUESTRA): Normalization of relaxation and RF irradiation spillover effects for improved quantitative chemical exchange saturation transfer (CEST) MRI *Magnetic Resonance in Medicine.* 2011;67:936–942.

31 Sun Phillip Zhe. Simultaneous determination of labile proton concentration and exchange rate utilizing optimal RF power: Radio frequency power (RFP) dependence of chemical exchange saturation transfer (CEST) MRI *Journal of Magnetic Resonance.* 2010;202:155–161.

32 Wu Renhua, Xiao Gang, Zhou Iris Yuwen, Ran Chongzhao, Sun Phillip Zhe. Quantitative chemical exchange saturation transfer (qCEST) MRI – omega plot analysis of RF-spillover-corrected inverse CEST ratio asymmetry for simultaneous determination of labile proton ratio and exchange rate *NMR in Biomedicine.* 2015;28:376–383.

33 Meissner Jan-Eric, Goerke Steffen, Rerich Eugenia, et al. Quantitative pulsed CEST-MRI using Ω-plots *NMR in Biomedicine.* 2015;28:1196–1208.

34 Zaiss Moritz, Xu Junzhong, Goerke Steffen, et al. Inverse Z-spectrum analysis for spillover-, MT-, and T1-corrected steady-state pulsed CEST-MRI – application to pH-weighted MRI of acute stroke *NMR in Biomedicine.* 2014;27:240–252.

35 Roeloffs Volkert, Meyer Christian, Bachert Peter, Zaiss Moritz. Towards quantification of pulsed

494 spinlock and CEST at clinical MR scanners: an analytical interleaved saturation–relaxation
495 (ISAR) approach *NMR in Biomedicine.* 2014;28:40–53.

496 36 Santyr Giles E, Fairbanks E Jefferson, Kelcz Frederick, Sorenson James A. Off-resonance spin
497 locking for MR imaging *Magnetic Resonance in Medicine.* ;32:43–51.

498 37 Hwang T L, Shaka A J. Water Suppression That Works. Excitation Sculpting Using Ar-
499 bitrary Wave-Forms and Pulsed-Field Gradients *Journal of Magnetic Resonance, Series A.*
500 1995;112:275–279.

501 38 Grzesiek Stephan, Bax Ad. The importance of not saturating water in protein NMR. Application
502 to sensitivity enhancement and NOE measurements *Journal of the American Chemical Society.*
503 1993;115:12593–12594.

504 39 Geen Helen, Freeman Ray. Band-selective radiofrequency pulses *Journal of Magnetic Resonance*
505 *(1969).* 1991;93:93–141.

506 40 Cavanagh John, Fairbrother Wayne J., Palmer III Arthur G., Rance Mark, Skelton Nicholas J..
507 *Protein NMR spectroscopy.* Elsevier Academic Press2nd ed. 1996.

508 41 Zhang Ouwen, Kay Lewis E, Olivier J Paul, Forman-Kay Julie D. Backbone 1H and 15N res-
509 onance assignments of the N-terminal SH3 domain of drk in folded and unfolded states us-
510 ing enhanced-sensitivity pulsed field gradient NMR techniques *Journal of Biomolecular NMR.*
511 1994;4:845–858.

512 42 Seber G. A. F., Wild C. J.. *Nonlinear Regression* . 1989.

513 43 Bassi Roberto, Niewczas Monika A, Biancone Luigi, et al. Metabolomic Profiling in Individuals
514 with a Failing Kidney Allograft *PloS one.* 2017;12:e0169077-e0169077.

515 44 Vold Robert L, Daniel E S, Chan S O. Magnetic resonance measurements of proton exchange in
516 aqueous urea *Journal of the American Chemical Society.* 1970;92:6771–6776.

517 45 Yavari Issa, Roberts John D.. Nitrogen-15 nuclear magnetic resonance spectroscopy. NH proton
518 exchange reactions of urea and substituted ureas *Organic Magnetic Resonance.* 1980;13:68–71.

519 46 Dortch R D, Horch R A, Does M D. Development, simulation, and validation of NMR relaxation-
520 based exchange measurements *The Journal of Chemical Physics.* 2009;131:164502.

47 Englander S W, Downer N W, Teitelbaum H. Hydrogen Exchange *Annual Review of Biochemistry.* 1972;41:903–924.

48 Wu Renhua, Liu Charng-Ming, Liu Philip K, Sun Phillip Zhe. Improved measurement of labile proton concentration-weighted chemical exchange rate (kws) with experimental factor-compensated and T1-normalized quantitative chemical exchange saturation transfer (CEST) MRI *Contrast Media & Molecular Imaging.* 2012;7:384–389.

49 Sun Phillip Zhe, Wang Yu, Dai ZhuoZhi, Xiao Gang, Wu Renhua. Quantitative chemical exchange saturation transfer (qCEST) MRI – RF spillover effect-corrected omega plot for simultaneous determination of labile proton fraction ratio and exchange rate *Contrast Media & Molecular Imaging.* 2014;9:268–275.

50 Bottomley Paul A., Griffiths John R.. *Handbook of magnetic resonance spectroscopy in vivo : MRS theory, practice and applications.* Wiley: Chichester, UK 2016.

51 Liu Lingyan, Mo Huaping, Wei Siwei, Raftery Daniel. Quantitative analysis of urea in human urine and serum by 1H nuclear magnetic resonance *Analyst.* 2012;137:595–600.

52 Valérie C Pierre Matthew J Allen. *Contrast Agents for MRI: Experimental Methods (New Developments in NMR).* Royal Society of Chemistry1st ed. 2017.

53 Zaiss Moritz, Bachert Peter. Exchange-dependent relaxation in the rotating frame for slow and intermediate exchange – modeling off-resonant spin-lock and chemical exchange saturation transfer *NMR in Biomedicine.* 2012;26:507–518.

54 Zaiss Moritz, Bachert Peter. Chemical exchange saturation transfer (CEST) and MR Z -spectroscopy in vivo : a review of theoretical approaches and methods *Physics in Medicine and Biology.* 2013;58:R221-R269.

55 Stabinska Julia, Cronenberg Tom, Wittsack Hans-Jörg, Lanzman Rotem Shlomo, Müller-Lutz Anja. Quantitative pulsed CEST-MRI at a clinical 3T MRI system *Magnetic Resonance Materials in Physics, Biology and Medicine.* 2017;30:505–516.

56 Pavuluri KowsalyaDevi, McMahon Michael T. pH Imaging Using Chemical Exchange Saturation Transfer (CEST) MRI *Israel Journal of Chemistry.* 2017;57:862–879.

548 57 Wu Yunkou, Zhang Shanrong, Soesbe Todd C, et al. pH imaging of mouse kidneys in vivo using
549 a frequency-dependent paraCEST agent *Magnetic Resonance in Medicine.* 2015;75:2432–2441.

550 58 Longo Dario Livio, Dastrù Walter, Digilio Giuseppe, et al. Iopamidol as a responsive MRI-
551 chemical exchange saturation transfer contrast agent for pH mapping of kidneys: In vivo studies
552 in mice at 7 T *Magnetic Resonance in Medicine.* 2010;65:202–211.

553 59 Longo Dario, L , Sun Phillip Zhe, et al. A General MRI-CEST Ratiometric Approach for pH
554 Imaging- Demonstration of in Vivo pH Mapping with Iobitridol *Journal of the American Chem-*
555 *ical Society.* 2014;136:14333–14336.

556 60 Sun Phillip Zhe, Longo Dario Livio, Hu Wei, Xiao Gang, Wu Renhua. Quantification of iopamidol
557 multi-site chemical exchange properties for ratiometric chemical exchange saturation transfer
558 (CEST) imaging of pH *Physics in Medicine and Biology.* 2014;59:4493–4504.

559 61 Finer E G, Franks F, Tait M J. Nuclear magnetic resonance studies of aqueous urea solutions
560 *Journal of the American Chemical Society.* 1972;94:4424–4429.

561 62 Chan Kannie W Y, McMahon Michael T, Kato Yoshinori, et al. Natural D-glucose as
562 a biodegradable MRI contrast agent for detecting cancer *Magnetic resonance in medicine.*
563 2012;68:1764–1773.

564 63 Hills B P. Multinuclear NMR studies of water in solutions of simple carbohydrates. *Molecular*
565 *Physics.* 1991;72:1099–1121.

566 64 Wiebenga-Sanford Benjamin P, DiVerdi Joseph, Rithner Christopher D, Levinger Nancy E.
567 Nanoconfinement's Dramatic Impact on Proton Exchange between Glucose and Water *The Jour-*
568 *nal of Physical Chemistry Letters.* 2016;7:4597–4601.

569 65 Lee Jae-Seung, Xia Ding, Jerschow Alexej, Regatte Ravinder R. In vitro study of endogenous
570 CEST agents at 3 T and 7 T *Contrast Media & Molecular Imaging.* 2015;11:4–14.

571 66 Haris Mohammad, Cai Kejia, Singh Anup, Hariharan Hari, Reddy Ravinder. In vivo mapping
572 of brain myo-inositol *NeuroImage.* 2011;54:2079–2085.

573 67 Liepinsh Edvards, Otting Gottfried. Proton exchange rates from amino acid side chains— im-
574 plications for image contrast *Magnetic Resonance in Medicine.* 2018;35:30–42.

575 68 Wermter Felizitas C, Bock Christian, Dreher Wolfgang. Investigating GluCEST and its specificity
576 for pH mapping at low temperatures *NMR in Biomedicine.* 2015;28:1507–1517.

577 69 Basharat Meer, deSouza Nandita M., Parkes Harold G., Payne Geoffrey S.. Determining the
578 chemical exchange saturation transfer (CEST) behavior of citrate and spermine under in vivo
579 conditions *Magnetic Resonance in Medicine.* 2016;76:742–746.

580 70 DeBrosse Catherine, Nanga Ravi Prakash Reddy, Bagga Puneet, et al. Lactate Chemical Ex-
581 change Saturation Transfer (LATEST) Imaging in vivo A Biomarker for LDH Activity *Scientific*
582 *reports.* 2016;6:19517.

583 Figures and Tables

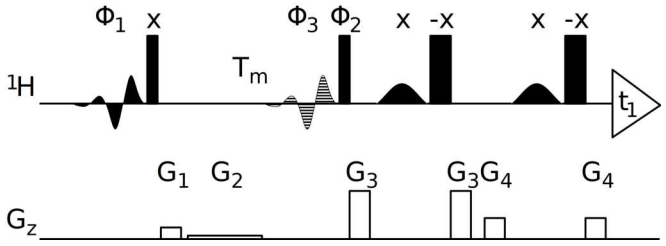

Figure 1: WEX II pulse sequence with excitation sculpting and water flip-back. Narrow and wide bars are hard rectangular 90° and 180° pulses, respectively, applied at maximum permissible amplifier power with the phase indicated above each pulse. Water-selective 90° pulses have an E-BURP-1 shape (39) and a duration of 12.0 ms (at 600 MHz). Water-selective 180° pulses have a shape corresponding to the central lobe of a sinc function and a duration of 4.0 ms. The basic phase cycle of the WEX II sequence is ϕ_1: x,-x,x,-x; ϕ_2: x,x,-x,-x; ϕ_3: x,-x,-x,x; receiver: x,-x,-x,x and is expanded by EXORCYCLE phase cycling of the 180° pulses in the excitation sculpting sequence.The pulsed field gradients are G_1: 10 G/cm, 1.0 ms; G_2: 1 G/cm; G_3: 43 G/cm, 0.5 ms; G_4: 19 G/cm, 0.5 ms.

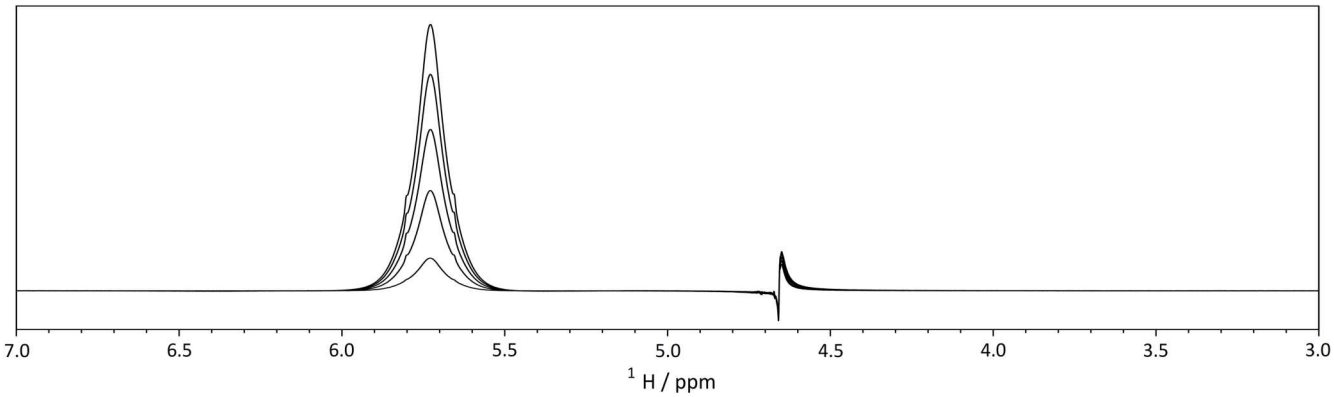

Figure 2: Overlay of the 1D ^{1}H WEX II spectra recorded using the pulse sequence shown in Figure 1 at pH 6.96 and 37.0°C with T_m = 20.0 ms, 40.0 ms, 60.0 ms, 80.0 ms, and 100.0 ms (from bottom to top). Due to scalar relaxation of the second kind caused by the fast quadrupolar relaxation of the most abundant nitrogen isotope ^{14}N the urea ^{1}H resonance is very broad (61); the ^{15}N satellites cause a doublet separated by the scalar coupling $^{1}J_{NH}$ which is visible as shoulders on the main ^{1}H resonance of urea. Excitation sculpting with water flip-back results in highly efficient suppression of the residual $^{1}H_2O$ resonance at approximately 4.66 ppm with a very flat baseline. Magnetization transfer to the urea resonance due to water exchange is approximately linear with the effective mixing time in the initial slope regime, but due to the effects of the water flip-back pulse in Figure 1 the effective mixing time ($T_m - T_{WFB}$) is systematically shorter than T_m, which is reflected in the disproportionally weak intensity of the urea resonance for T_m = 20.0 ms.

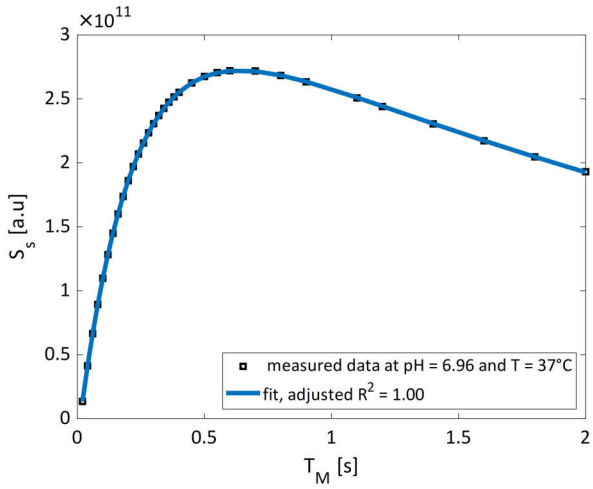

Figure 3: Integrated signal intensities S_s of the urea peaks (squares) at pH = 6.96 and $T = 37.0°C$ as a function of mixing time T_m, and the fit function $S_s(T_m - T_{WFB})$ (Equation 3) (solid blue line).The quality of the fit was $R^2 = 1.00$.

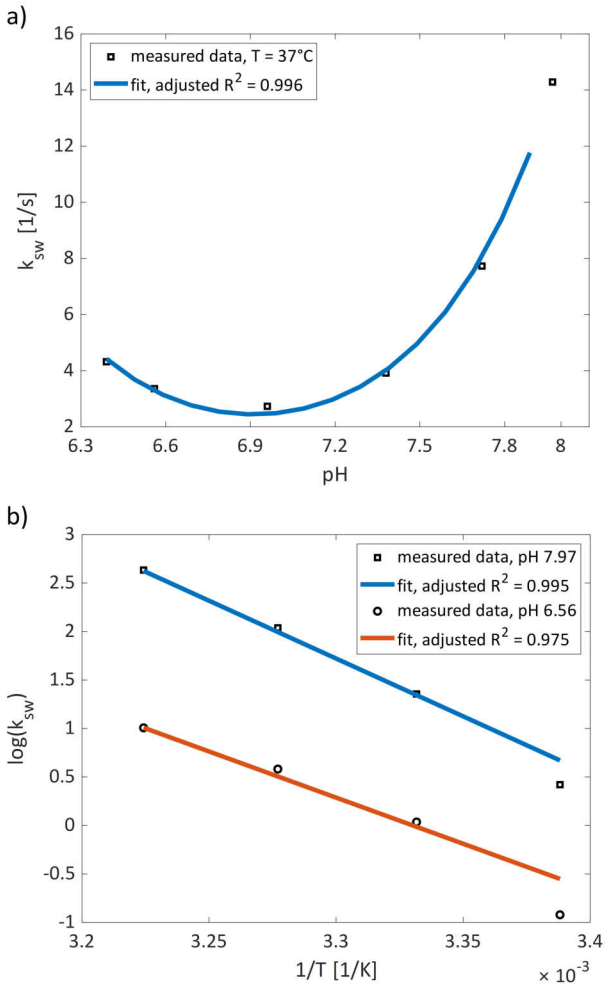

Figure 4: Determined k_{sw} (squares) values of urea as a function of (a) pH and (b) temperature.(a) Temperature $T = 37.0°\text{C}$ and urea concentration $c_{urea} = 250$ mM were fixed. Data were fitted using Equation 4 (solid blue line) yielding the following parameters: $k_b = (6.21 \pm 0.21) \times 10^6$ l/mol ·s, $k_a = (9.95 \pm 1.11) \times 10^6$ l/mol ·s and $R_{1s} = (1.90 \pm 0.31) s^{-1}$ ($R^2 = 0.996$).(b) Arrhenius plot from data measured at fixed urea concentration $c_{urea} = 250$ mM at pH 7.97 (square) and pH 6.56 (circle). Data were fitted using Equation 5 (solid blue line) and 6 (solid yellow line) yielding the following values of activation energies: $E_{A,b} = 43.52 \pm 9.56$ kJ/mol (R^2 =0.995) and $E_{A,a} = 79.13 \pm 15.87$ kJ/mol ($R^2 = 0.975$).

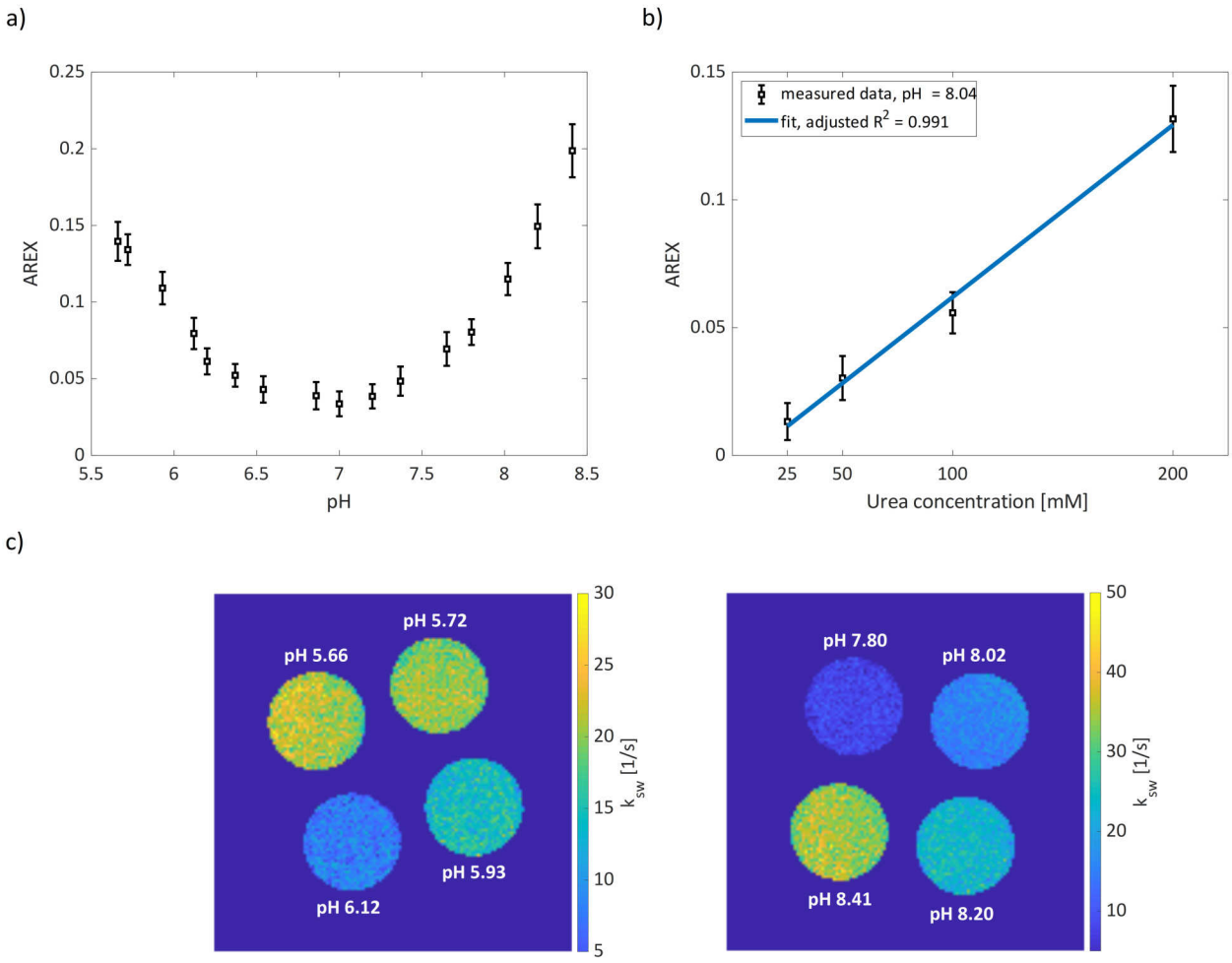

Figure 5: Apparent exchange-dependent relaxation (AREX) as a function of (a) pH and (b) urea concentration c_{urea} and (c) two exemplary exchange rates k_{sw} maps.(a) Temperature T = (37 ± 1)°C and urea concentration c_{urea} = 250 mM were fixed. The AREX values were obtained from Equations 8 and 9 (b) Temperature T = (37 ± 1) °C and pH_{fixed} = 8.04 were fixed. Data were fitted (solid blue line) using Equations 8, 9 and 11. The fit quality was: R^2 = 0.991. (c) The k_{sw} maps for two sets of the urea model solutions: #1 (pH 5.66, c_s = 250 mM), #2 (pH 5.72, c_s = 250 mM), #3 (pH 5.93, c_s = 250 mM), #4 (pH 6.12, c_s = 250 mM), #5 (pH 7.80, c_s = 250 mM), #6 (pH 8.02, c_s = 250 mM), #7 (pH 8.20, c_s = 250 mM), #8 (pH 8.41, c_s = 250 mM) obtained from the quantitative CEST experiments at T = 37°C.

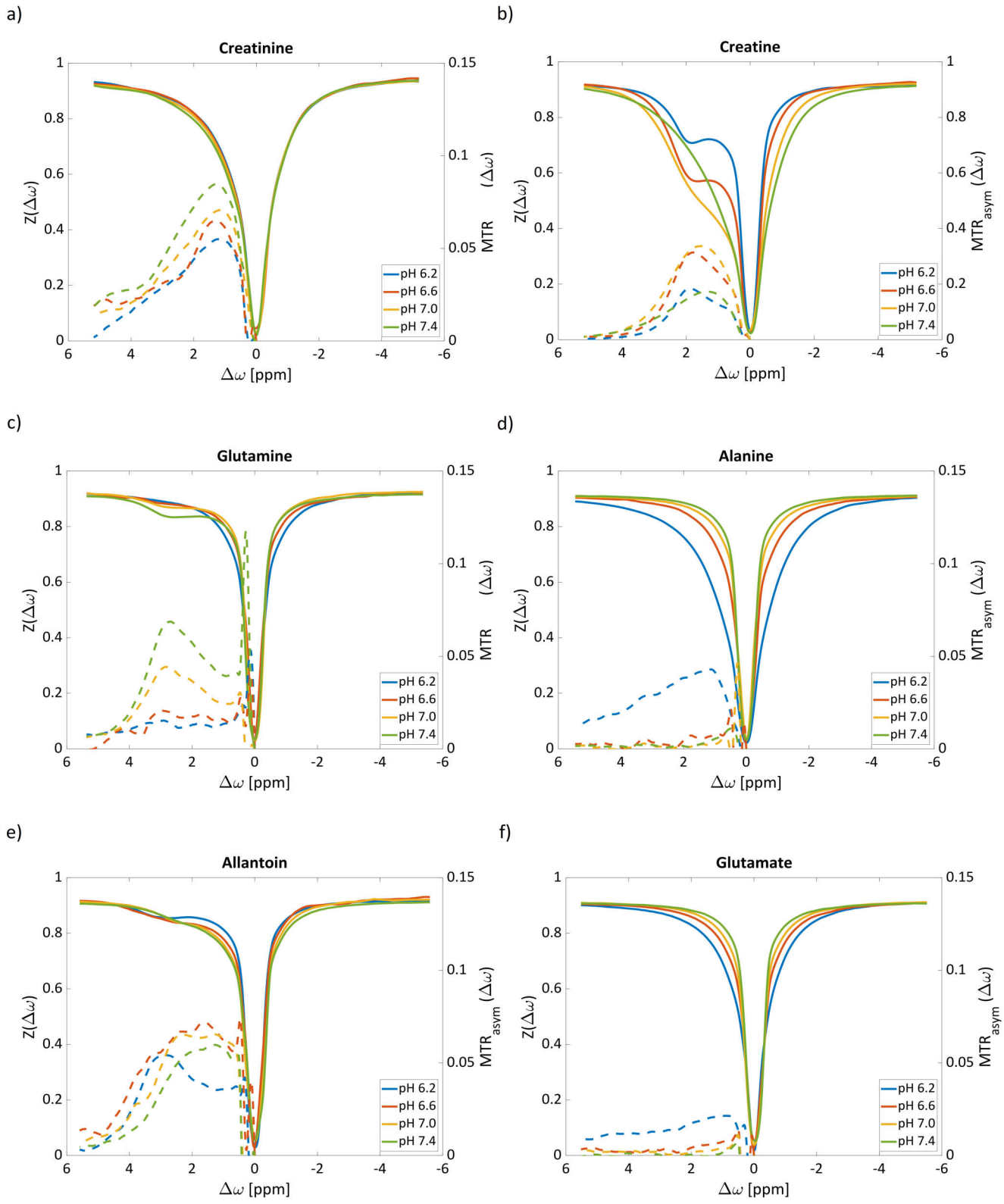

Figure 6: Experimentally obtained z-spectra (solid lines) and MTR_{asym} curves (dashed lines) of different kidney metabolites at $T = 37°C$. The metabolites are: a) creatinine (100 mM), b) creatine (100 mM), c) glutamine (100 mM), d) alanine (100 mM), e) allantoin (35 mM), f) glutamate (50 mM).

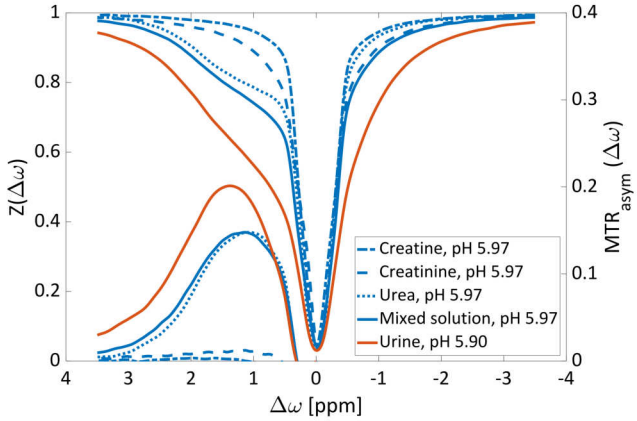

Figure 7: Z-spectra and MTR_{asym} curves for the individual solutions of 180 mM urea (blue dotted line), 15 mM creatinine (blue dashed line), 1 mM creatine (blue dash-dot line), their mixture (blue solid line) at pH 5.97 and for the urine sample (red solid line) at pH 5.90. The temperature of the model solutions during the measurements was kept constant at $T = (37 \pm 1)$°C.

Table 1: $k_{sw} + R_{1s}$ [1/s] and R_{1w} [1/s] values in urea aqueous solutions (c_s = 250 mM) measured by WEX at different pH and temperatures. The standard errors are approximately 0.04% and R^2 = 1.0

pH	T [°C]	R_{1w} [1/s]	$k_{sw} + R_{1s}$ ([1/s])
6.39	37.0	0.29	6.22
6.56	22.0	0.39	2.92
6.56	27.0	0.35	3.56
6.56	32.0	0.33	4.31
6.56	37.0	0.31	5.26
6.96	37.0	0.30	4.63
7.38	37.0	0.30	5.82
7.72	37.0	0.30	9.63
7.97	22.0	0.38	3.78
7.97	27.0	0.35	6.14
7.97	32.0	0.32	9.93
7.97	37.0	0.30	16.19

Table 2: Exchange rate k_{sw} [1/s] values in urea model solutions ($c_s = 250$ mM) obtained from CEST at different pH and $k_{sw,ref}$ estimated from WEX by extrapolation of Equation [5].

pH	T [°C]	k_{sw} $[1/s]$	$k_{sw,ref}$ $[1/s]$
5.66	37 ± 1	21.10 ± 2.80	21.84
5.72	37 ± 1	19.92 ± 2.20	19.04
5.93	37 ± 1	14.38 ± 2.33	11.82
6.12	37 ± 1	7.87 ± 2.25	7.75
6.20	37 ± 1	3.88 ± 1.88	6.51
7.37	37 ± 1	1.04 ± 2.10	4.60
7.65	37 ± 1	5.66 ± 2.41	6.92
7.80	37 ± 1	8.07 ± 1.85	9.61
8.02	37 ± 1	15.68 ± 2.31	15.80
8.20	37 ± 1	23.26 ± 3.14	23.83
8.41	37 ± 1	34.11 ± 3.81	38.58

Table 3: An overview of important kidney metabolites and their CEST properties

Compound	Functional group	δ_s [ppm][1]	k_{sw}[1/s][2]	c_s in urine[3, (19)]
Sugars	Hydroxyl protons (-OH)			
Glucose	-OH	1.2, 2.2, 2.8[(62)]	∼2000[(63), (64)]	37.5 (12.5-58.4)
Sorbitol	-OH	1.0[(7)]	n/a	9.9 (2.5-18.7)
Glycogen	-OH	1.2, 2.2, 3.0[(65)]	∼600[(65)]	n/a
Myo-inositol	-OH	∼0.8, ∼0.9, ∼1.1[(65)]	600[(66)]	22.4 (7.9-36.1)
Amino acids	Amino protons (-NH_2)			
Creatinine	-NH_2	∼1.3	n/a	14743±9797[4]
Creatine	Guanidinium protons	1.9	∼490[5, (55)]	46 (3-448)
Histidine	-NH_2, -NH	n/a	n/a, 1700[6, (67)]	43 (17-90)
Glutamine	-NH_2	2.9	n/a	37.3 (19.1-77.9)
Alanine	-NH_2	3.0[(7)]	∼3030[7, (68)]	21.8 (7.1-43.1)
Lysine	-NH_2	3.0[(7)]	4000[6, (67)]	17.2 (3.7-51.3)
Threonine	-NH_2, -OH	n/a, n/a	n/a, 700[6, (67)]	13.3 (6.4-25.2)
Glutamate	-NH_2	∼3.0	∼2000[9, (65)]	8.5 (3.3-18.4)
Miscellaneous				
Urea	-NH_2	1.0	∼1	12285 (174-49097)
Ammonia	NH_3	2.4[(13)]	n/a	1900.0 ± 350.0
Hippuric acid	-OH, -NH	n/a, n/a	n/a, n/a	229 (19-622)
Citric acid	-OH	0.6-0.8[(69)]	>2000[(69)]	203 (49-600)
Taurine	-NH_2	∼3.0[(65)]	300[8, (65)]	81 (13-251)
Allantoin	-NH_2, -NH	∼1.0, ∼3.0	n/a, n/a	15.4 (4.9-29.3)
Lactate	-OH	0.4[(70)]	350[9, (70)]	11.6 (3.5-29.3)
Choline	-OH	∼1.0[(65)]	∼400[(65)]	3.5 (1.4-6.1)

[1] δ_s in ppm is relative to the resonant frequency of water.

[2] Measured at pH 7.4 and at T = 25°C unless otherwise noted.

[3] Concentrations of all compounds are given in [μM/mM creatinine] unless otherwise noted.

[4] μM

[5] Measured at pH 7.51.

[6] Measured at pH 7.0 and T = 36°C.

[7] Measured at pH 7.0 and T = 22°C.

[8] Measured at pH 5.6.

[9] Measured at pH 7.0.